SCIENCE CHINA
Earth Sciences

•RESEARCH PAPER•

October 2018 Vol.61 No.10: 1510–1522
https://doi.org/10.1007/s11430-017-9237-4

Human-induced changes in recent sedimentation rates in Bohai Bay, China: Implications for coastal development

Fu WANG[1,2*], Lizhu TIAN[1,2], Xingyu JIANG[1,2], William MARSHALL[3] & Hong WANG[1,2]

[1] *Tianjin Center, China Geological Survey (CGS), Tianjin 300170, China;*
[2] *Key Laboratory of Muddy Coast Geo-Environment, China Geological Survey, Tianjin 300170, China;*
[3] *Plymouth University, Plymouth, Devon PL4 8AA, United Kingdom*

Received August 1, 2017; revised February 27, 2018; accepted June 14, 2018; published online September 5, 2018

Abstract In many countries, coastal planners strive to balance the demands between civil, commercial strategy and environmental conversation interests for future development, particularly given the sea level rise in the 21st century. Achieving a sustainable balance is often a dilemma, especially in low-lying coastal areas where dams in inland river basin are trapping significant amounts of fluvial sediments. We recently investigated the shore of Bohai Bay in northern China where there has been a severe increase in sea level following a program of large-scale coastal reclamation and infrastructure development over the last five decades. To investigate this trend, we obtained sediment cores from near-shore in Bohai Bay, which were dated by ^{137}Cs and ^{210}Pb radionuclides to determine the sedimentation rates for the last 50 years. The average sedimentation rates of Bohai Bay exceeded 10 mm yr^{-1} before 1963, which was much higher than the rate of local sea-level rise. However, our results showed an overall decreasing sedimentation rate after 1963, which was not able to compensate for the increasing relative sea-level rise in that period. In addition, our results revealed that erosion occurred after the 1980s in the shallow sea area of Bohai Bay. We suggest that this situation places the Bohai Bay coast at a greater risk of inundation and erosion within the next few decades than previously thought, especially in the large new reclamation area. This study may be a case study for many other shallow sea areas of the muddy coast if the sea level continues to rise rapidly and the sediment delivered by rivers continues to decrease.

Keywords ^{210}Pb, ^{137}Cs, Sedimentation rate, Reclamation, Coast, Tianjin

Citation: Wang F, Tian L, Jiang X, Marshall W, Wang H. 2018. Human-induced changes in recent sedimentation rates in Bohai Bay, China: Implications for coastal development. Science China Earth Sciences, 61: 1510–1522, https://doi.org/10.1007/s11430-017-9237-4

1. Introduction

In many countries, large sections of the coastal zone, prized for their high commercial and strategic value, are subject to intensifying pressures from human occupation and global climate warming, a direct driver of higher sea levels. However, the narrow coastal strip with limited natural resources does not always support the increasing demands from human activity (Martínez et al., 2007; James et al., 2009; Syvitski, 2012).

The shore of Bohai Bay (Figure 1) is currently experiencing the 'coastal squeeze' due to the pressures from both sea-level rise and intensifying human impact. Compared to the early 20th century, the urban area of Tianjin city has expanded approximately 10-fold, reaching ca. 250 km^2 (Zhong and Kang, 2002). By 2012, there were >14 million residents in the Tianjin metropolitan area (Tianjin Bureau of Statistics, 2013). The highest rate of urban expansion has occurred during the last decade (Zhang et al., 2010) when the Tianjin-Binhai-New-Area was created. Due to this coastal development, extensive tracts of intertidal and shallow nearshore area around the bay coast have been reclaimed, creating nearly 300 km^2 of new land since 2003 (Wang et al., 2010). This reclaimed area has multifaceted values, but these can be

* Corresponding author (email: wfu@cgs.cn)

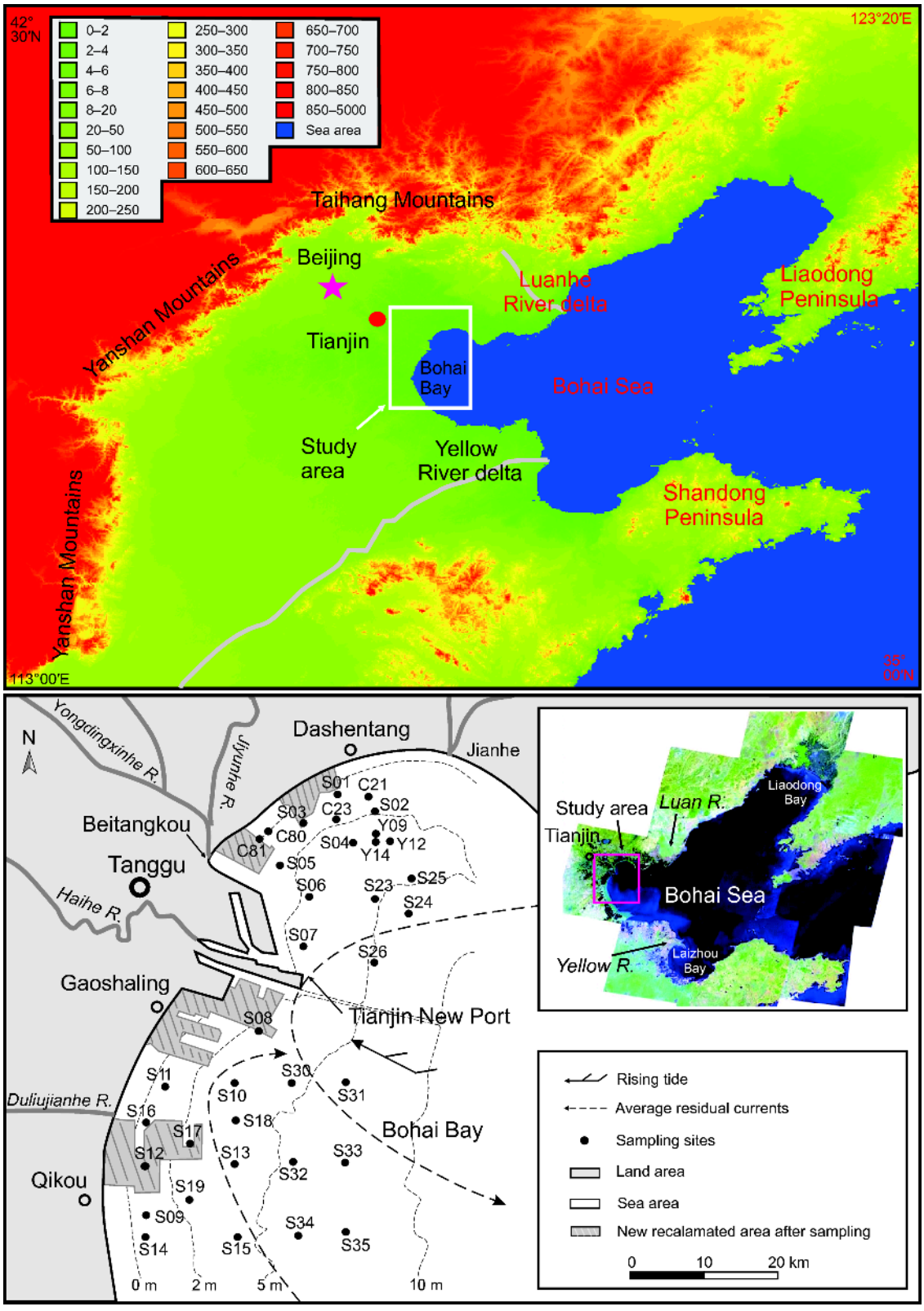

Figure 1 The geographic location of Bohai Bay and the short core sites. Also shown is the claimed coastal area (hatched blocks) during 2009–2015. The base map data were generated using the open and free software DIVA-GIS 7.5 (http://www.diva-gis.org/).

overlooked when coastal management plans are conceived with narrow commercial objectives. Notably, the presence of intertidal wetland can act as a natural buffer to alleviate possible damage from extreme storm events and coastal

flooding resulting from changing climate and rising sea levels (Sardá et al., 2005; IPCC, 2013).

In this region, dam construction and channel modifications in the upper stream of the river basins during the last sixty years has reduced dramatically the riverine sediment load to the estuaries (Blum and Roberts, 2009; Ericson et al., 2006). In the study area, there are seven rivers from the west feeding into Bohai Bay (Figure 1). At present the Haihe supplies approximately 1.8×10^5 t yr^{-1}, the Yellow River 1.1×10^9 t yr^{-1} and Luanhe River 2.7×10^7 t yr^{-1}. The Haihe used to supply 6×10^6 t yr^{-1} before the construction of a dam upstream in 1958 (Qin et al., 1990). The runoff of the Haihe decreased as follows: 729.9×10^8 m^3 during the 1950s→436×10^8 m^3 during the 1960s→100.9×10^8 m^3 during the 1970s→and 17.0×10^8–28.4×10^8 m^3 since the 1980s. The Beitang estuary and Duliujianhe estuary show the same decrease in runoff trend (Lei et al., 2007). These data show that runoff is virtually absent during dry years due to dam construction on its river system in the 1950s–1960s. The sediment discharge by the Haihe decreases from 5213×10^4 t in the 1950s to 360×10^4 t in the 1970s (Hu and Qi, 2000). The suspended sediment flux of the Luanhe River declined to only 9% of the levels before the construction of the two large dams in 1979 (Xue et al., 2009).

All our coastlines are facing continuing rising sea level. From 1980 to 2016, the average absolute sea level rise rate along the coast of China was 3.0 mm yr^{-1} (SOA, 2017). The rate on the Tianjin coast was slightly higher, and reached 3.4 mm yr^{-1} based on the raw tidal data from 1959–2008 from Tanggu marine environment monitoring stations in Tianjin New Port (Li et al., 2011). However, Wang et al. (2013) contend that the sea level rising rate of Tianjin was 2.7 mm yr^{-1} from 1950–2010 (Wang et al., 2013), and it is suggested that the rate of the sea level rise has accelerated during the last 30 years to 3.8 mm yr^{-1}. Furthermore, latest results show that the sea level increase rate reached 7.7 mm yr^{-1} in the last ten years (Bi et al., 2013).

It is established (e.g., Li et al., 2011; Bi et al., 2013) that the developed Bohai Bay coastal area is subject to ongoing rising sea level, and a reduced supply of river transport sediments (Hu and Qi, 2000; Xue et al., 2009). Therefore, the fundamental question of whether any increase in development in the Bohai Bay coastal zone is sustainable is becoming more and more important. In this paper, dating of short cores collected from the shallow sea (0−10 m water depth) of Bohai Bay is used to discuss the dynamic and complex relationship between the nearshore sediment flux and sea level rise and the potential impact of an extensive program of commercial development, land reclamation and shoreline geo-engineering on the Bohai Bay coast (Figure 1). Given the predicted global sea-level rise (to 0.98 m) by the end of the 21st century (IPCC, 2013), this study attempts to answer the question of whether the Bohai Bay coast is sustainable.

2. Study area

Bohai Bay in northern China is a large semi-enclosed sea, connected to the Pacific through a gap between the two peninsulas (Shandong peninsula and Liaoning peninsula), and the Yellow Sea. It has a coast line of >200 km and a water surface area of ca. 15900 km^2 (Figure 1). The mean water depth in the Bay is 12.5 m, and the mean tidal range is 2.4 m at the Port of Tianjin (China Communications First Design Institute of Navigation Engineering and National Marine Data and Information Service, 2006).

There are significant fluvial inputs and the bay lies between two deltaic plains, the Yellow River in the south and the Luan River in the north (Figure 1). The coastal lowland is characterized by not only its low-lying nature, i.e. less than 10 m above sea level, but also the development of a series of Chenier ridges associated with the Yellow River discharge since later Holocene (e.g. Su et al., 2011), and buried oyster reefs north of the Haihe River (e.g. Wang et al., 2011). Several small rivers, including the Haihe and the Duliujianhe, flow through the lowland and enter the Bay. Due to the low gradient of the coast, the shoreline retreated to the continental margin of the Yellow Sea, more than 1000 km to the east and southeast, during the Last Glacial Maximum (e.g. He, 2006). During the Holocene, the sea inundated the coastal area and penetrated about 80 km inland from the current shoreline (e.g. Wang et al., 2015).

Two coastal currents from north and south, respectively, converge off the shore of Tianjin and flow eastwards back to the sea (Zhao et al., 1995). Tianjin New Port was founded in 1939, but the original port at Tianjin opened in 1860, and it was the earliest to engage in significant foreign trade in this region. Sediments from Haihe spread along the coast to the north and south, and move offshore and out of the bay, however, following the construction of the latest breakwaters protecting the new port of Tianjin, sediment from Haihe flows mostly southwestwards (Wang F et al., 2014). Since the 1960s, freshwater and riverine sediment flux discharging into the bay has been significantly reduced due to water extraction and the construction of dams in the catchments (Hu and Qi, 2000). It is evident that the Bohai Bay coastline has stopped progradation, and instead undergoes siltation flooded by tidal currents intensified by marine processes (Zhong and Kang, 2002; Wang, 2003; Li et al., 2007).

3. Material and methods

3.1 Sampling

In 2007–2010, 36 sediment cores, 60–110 cm long, were taken from the nearshore sea bed in the Bohai Bay using a gravity corer (Figure 1). After recovery, the cores were stored vertically in a plastic tube before slicing into 4 cm

segments in the laboratory for radionuclide measurement and particle size analysis. The radionuclide sub-samples were dried, disaggregated and packed in an airtight container and stored for >30 days, ensuring radioactive equilibrium between ^{226}Ra and its daughter ^{222}Rn (half-life of 3.8 days).

3.2 Principles and radionuclide analysis

The activities of the radionuclides ^{210}Pb, ^{137}Cs, and ^{226}Ra (by way of its granddaughter ^{214}Pb) were measured using a gamma spectrometry utilizing the photon energies at 46.5, 662, and 295+352 keV, respectively. The $^{210}Pb_{exc}$ fraction was calculated by subtracting ^{226}Ra (^{214}Pb) from the total ^{210}Pb activity. The activates in sub-samples of 10 g dry weight in the cores S11–S19, C21, C23, C80 and C81 were measured using a GWL-120-15, ORTEC well detector housed at the Nanjing Institute of Geography & Limnology, Chinese Academy of Sciences (NIGL, CAS). The well detector was calibrated using radioisotope standard samples from Environmental Radioactivity Research Centre of the University of Liverpool and the IAEA. Additional sub-samples of 50 g dry weight taken from the core S01–S10, Y9, Y12, Y14, S23–S26, S30–S35, were measured using a Hyperpure coaxial Germanium detector (GMX60-15, ORTEC) housed at the Young Sediments Dating Lab, Tianjin Center, China Geological Survey. This instrument was calibrated using radioisotope standard samples from the Chinese Atomic Energy Institute and NIGL, CAS.

The first detectable ^{137}Cs activity in undisturbed sediment profiles has been previously proposed to mark the appearance of significant bomb-derived ^{137}Cs fallout in global environments in 1954 (Cambray et al., 1989; Callaway et al., 1996; Le Roux and Marshall, 2010). The global fallout of ^{137}Cs reached its maximum during the height of atmospheric tests from 1962–1964 (Cambray et al., 1989). Later, weapons tests produced reduced ^{137}Cs fall-out peaks in the years 1968−1979 (Mishra et al., 1975; Jha et al., 2003), and a significant regional fall-out event resulted from the 1986 reactor fire at Chernobyl in the Ukraine (Callaway et al., 1996; Le Roux and Marshall, 2010). Therefore, if the first presence of ^{137}Cs at depth (corresponding to age of 1954) or other unique peaks (e.g., corresponding to an age of 1963) can be identified the vertical profile of ^{137}Cs can be used to calculate average sedimentation rates. This approach has been widely used in other sediment cores (Delaune et al., 1978; Callaway et al., 1996; Goodbred and Kuehl, 1998; Radakovitch et al., 1999; Andersen et al., 2000; Su and Huh, 2002; Gehrels et al., 2006; Marshall et al, 2007; Wei et al., 2007; Irabien et al., 2008; Wang F et al., 2014; Wang et al., 2016b, 2016c), and we use this method to date our sediments. Following on, the sedimentation rates since 1963 were calculated based on the detected depth of ^{137}Cs peak (sedimentation rates=peak depth/(sampling time–1963)), and the average sedimentation rate during the year of 1954–1963 was also calculated (sedimentation rates=(maximum depth–peak depth)/(1963–1954)).

For $^{210}Pb_{exc}$ data, the CIC model is adopted to the calculation of the linear sedimentation rate for many marine sediments, which assume a constant initial concentration of $^{210}Pb_{exc}$ per unit dry weight at each stage of accumulation, despite variations in accumulation rates.

The sedimentation rate is calculated using equation below:

$$S = \lambda D / \ln(C_0 / C), \quad (1)$$

where S is sedimentation rates (cm yr^{-1}); λ is the decay constant for ^{210}Pb (λ=0.031 yr^{-1}); D is depth to z (cm); C_0 is the activity of the top layer of sediments (dpmg^{-1} or Bq kg^{-1}); and C is the activity of the sediments at depth z layer (dpm g^{-1} or Bq kg^{-1}).

3.3 Particle size analysis

All samples were processed with 10–20 mL of 30% H_2O_2 to remove organic matter, washed with 10% HCl to remove carbonates and shell fragments, and rinsed with deionized water. After processing, all samples were gently disaggregated in an ultrasonic vibrator for several minutes to facilitate dispersion in the analyzer. The grain size distribution of core sediment samples was analyzed using a laser particle analyzer (Microtrac S3500 Particle Size Analyzer) at the Tianjin Center of Geological Survey with a measuring range of 0.3–2000 μm. The grain size parameters were calculated according to the moment method (McManus, 1988).

4. Results

4.1 Particle size distribution

The range of sand, silt and clay content for cores S01–S04, S23–S25, and Y9, Y12, Y14 were 12.9–54.4%, 12.9–28.1% and 32.7–62.1%, respectively (Figure 2). The other cores had sand contents of 1.2–6.6% and clay and silt contents 25.5–39.4% and 59.4–68.1%, respectively.

The particle size distributions of the cores north of the Haihe, near the Beitang channel and in Tianjin Harbor, had an upward fining trend. The others had a coarsening trend based on average grain size (Figure 2). Notably, those cores taken south of the Haihe river (i.e., S32–S35, S09, S12, S14, S19) and in the nearshore sub-tidal shallows (0–10 m water depth). In addition, the cores from the Lvjuhe tidal flat had a strong upward coarsening trend (Figure 2).

4.2 Radionuclide activities and sedimentation rates

The $^{210}Pb_{exc}$ activity determined in the cores was low, most of the down-core profiles declined to background levels below 40 cm depth. Most cores had maximum activities

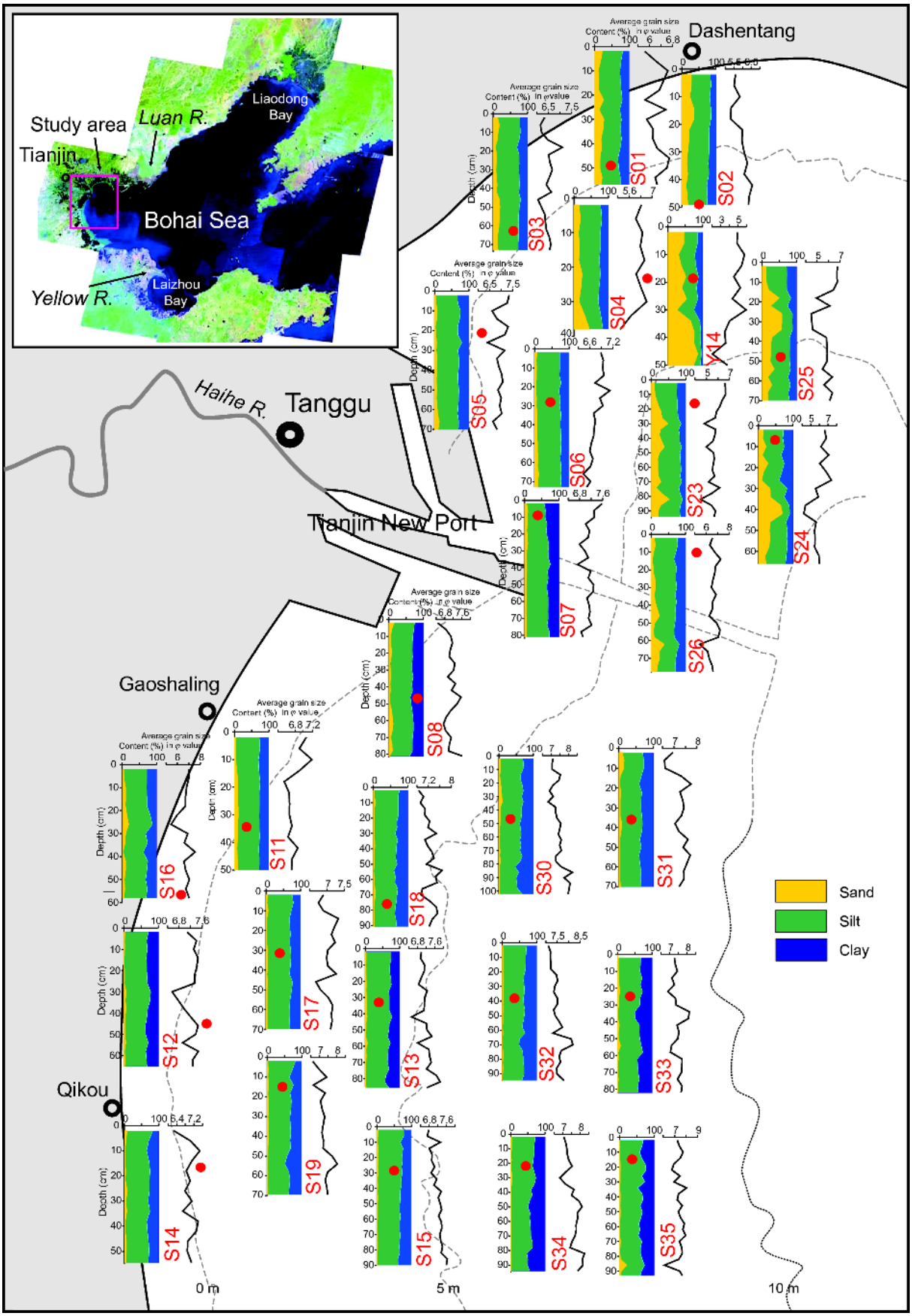

Figure 2 Particle size distribution of the cores.

<120 Bq kg^{-1}, and given the presence of lower values below this core depth or 40 cm and some reversed decay trends, we conclude that the inventories in many cores were the product of a systematic steady-state decay. Furthermore, considering the group core sample site, the down-core activity profiles did not follow a common trend (Figure 3). Significant variability occurred in the radionuclide inventories in individual cores within the same sampling zone (See Figure 1). Unfortunately, because of the low radionuclide activities and the non-systematic decay curves, it is impossible to simulate the sedimentation rates for cores based on $^{210}Pb_{exc}$. The values measured in these cores would be typically from sites where the uppermost younger sections had been eroded away. Alternatively, these values could result if the down-core sediment package was the product of the slow deposition of 'pre-aged' mature material, e.g., re-worked and transported from a distant source.

Wang et al. (2016c) reported that because of dam constructions in the rivers, sediment supply decreased since the 1960s. This change has led to sedimentary erosion and/or re-

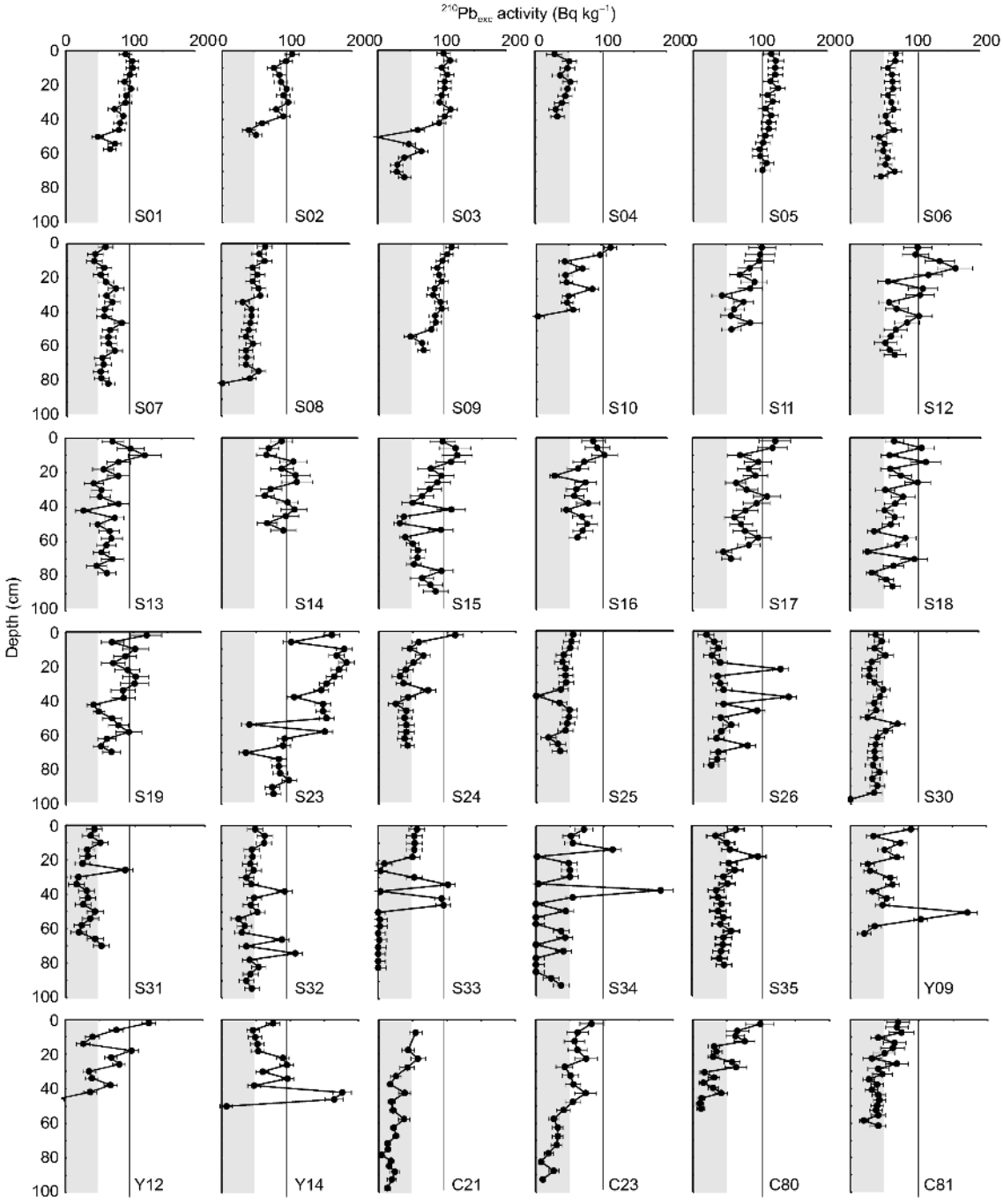

Figure 3 Depth profiles of $^{210}Pb_{exc}$ activity in the sediment cores. The gray shaded area is the activity level of <50 Bq kg^{-1}.

deposition in the subtidal area of Bohai Bay. These dams, and associated catchment disturbances, could be expected to influence the composition of the sediments transported. Since the 1980s, coastal engineering works have changed the sediment transport patterns, and triggered enhanced erosion in some locations. These changes in the sediment sources can also be expected to have some impact on the mineral composition, grain size and texture of the sediments reaching the near-shore zone of Bohai Bay. Changes in physical properties of the sediments will change the materials ability to retain individual radionuclides, and can result in a local fractionation following preferential retention, or loss, of a specific nuclide species (see Hormann and Fischer, 2013; Kabdyrakova et al., 2018 and references therein). We propose that this preferential retention may have happen in the sediments we find from Bohai Bay. In our sediments the $^{210}Pb_{exc}$ activity determined was low, and most of the down-core profiles declined to a low activity levels below 40 cm depth, preventing the production of any meaningful results for dating.

To explain this further, Figure 4 presents idealized depth distributions of $^{210}Pb_{exc}$ and ^{137}Cs activity profiles in our sediment-supply-decreasing environments. The profiles show the overestimated sedimentation rates based on $^{210}Pb_{exc}$ curves by mixing and erosion activity. Before 1950, the sedimentation rates were relatively high because the sediment supply was sufficient, and the $^{210}Pb_{exc}$ had a slow decay trend. After the 1950s, the sedimentation rates became low when the sediment supply decreased sharply following dam construction. Figure 4B shows the evidence of erosion and surface layer missing. Figure 4C shows the final measured profiles after erosion and mixing processes.

In contrast, the vertical profiles of ^{137}Cs activity detected in the sediments had structure, and most of the cores produced a similar curve. Although the maximum activity levels were all below 15 Bq kg^{-1}, most of the curves had a well-defined peak with steep rising and falling limbs (Figure 5). We interpret this peak as marking the level containing sediments deposited during the height of atmospheric nuclear weapons tests and date it at AD1963, this local peak was identified by the comparing study between ^{210}Pb and ^{137}C radionuclides and local hydro records (Wang et al., 2016a, 2016b, 2016c). This peak, or part of it, is observed in all the profiles except yj14. In cores S25, S31, S23 and S24, the falling limb is missing or is truncated, suggesting the younger sediments were missing. The first occurrence of ^{137}Cs at depth was not detected in cores S02, S04 and S26 because of the shortness of the cores. In core S02, only the falling limb was detected,

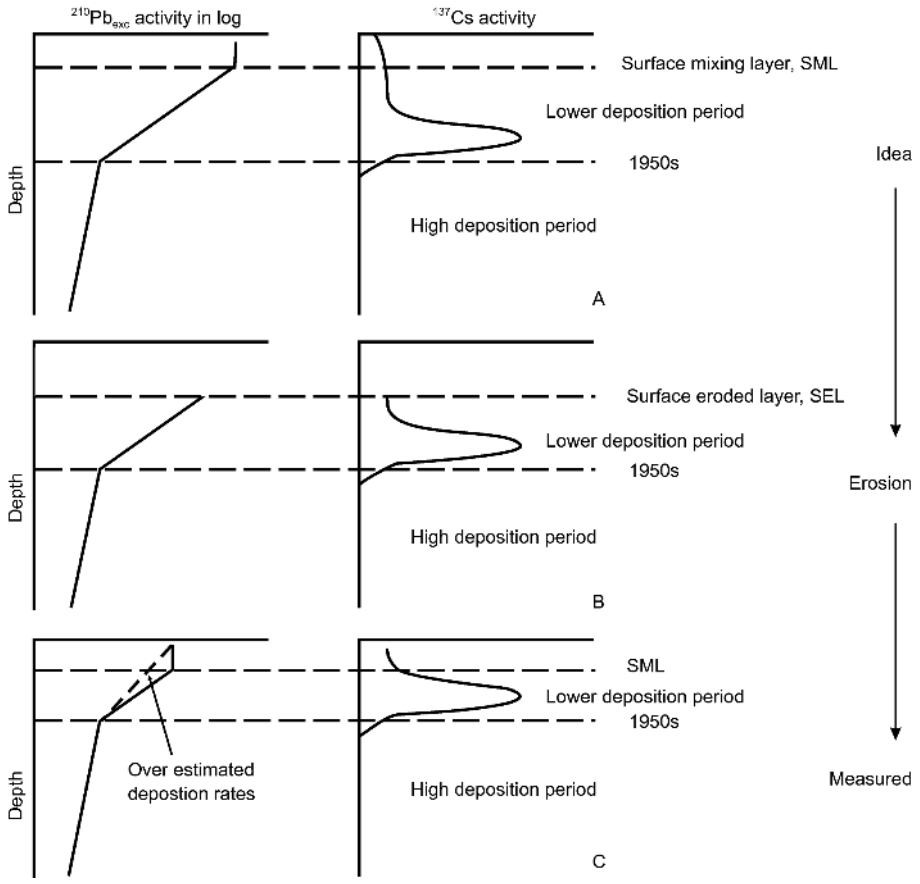

Figure 4 Vertical distribution of $^{210}Pb_{exc}$ and ^{137}Cs activity profiles in the shallow sea of Bohai Bay (Wang et al., 2016c).

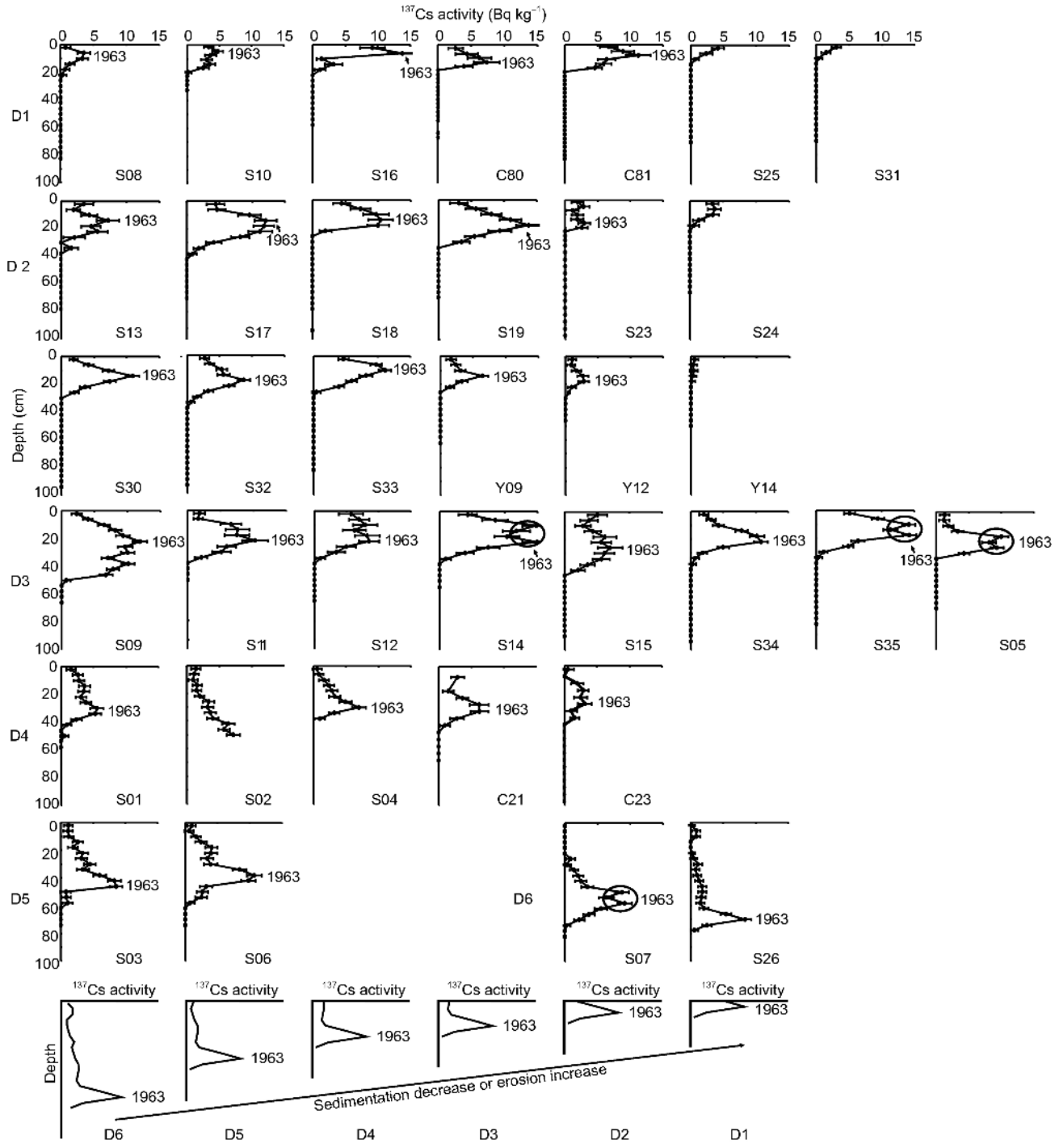

Figure 5 Depth profiles of ^{137}Cs in the sediment cores.

presumably because of the lack of recovery of deeper sediments.

For the other cores, the ^{137}Cs first occurrence depth and the peak depth can be identified obviously, the average sedimentation rates since 1954 were calculated based on maximum depths (sedimentation rates=maximum depth/(sampling time–1954)). Variability between area curves showed small variations in low-activity distribution patterns, but with approximately equivalent amplitudes, representing coarser sediments and associated stronger flow current environments. The sedimentation rates should be very low. The sedimentation rates in this study area were determined using both the ^{137}Cs profiles in the cores and dates modeled from the ^{210}Pb$_{exc}$ activity (Figure 6).

The results show that high sedimentation rates occurred during 1954 to 1963, and the maximum rates reached 2.0–2.9 cm yr^{-1},

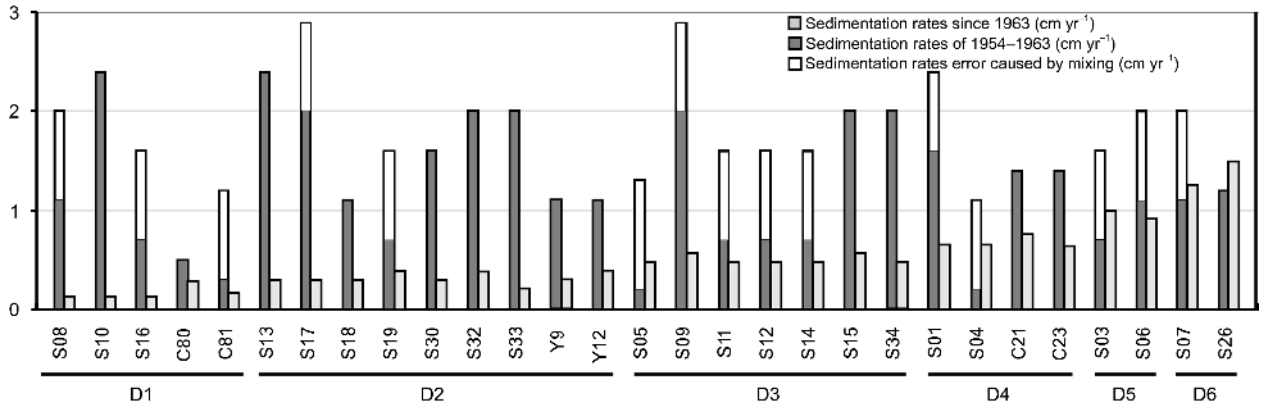

Figure 6 Histogram of the sedimentation rates calculated for each core.

located at sampling site 201017. The lowest rate was 0.17 cm yr^{-1}, located at sampling site CH81 after 1963.

4.3 Temporal and spatial variation of sedimentation rates

Although the mixing processes result in a large uncertainty in our estimation of sedimentation rates for the period 1954–1963, these can still be useful data. It can be concluded that the sedimentation rates from 1954 to 1963 are high; nearly all the rates are higher than 1 cm yr^{-1}, with the highest one reaching 2.9 cm yr^{-1}. Compared with the sedimentation rates of 1954–1963, the sedimentation rates decreased sharply in the late 1960s (Figure 6).

Figure 7 shows the spatial distribution of sedimentation rates dated by the peak of ^{137}Cs. Six districts can be identified based on the sedimentation rates, represented by D1–D6. D1 is distributed near 0–2 m water depth in south Haihe River, where the sedimentation rates are less than 0.2 cm yr^{-1}. D2 is distributed in the shallowest sea area of the south Haihe

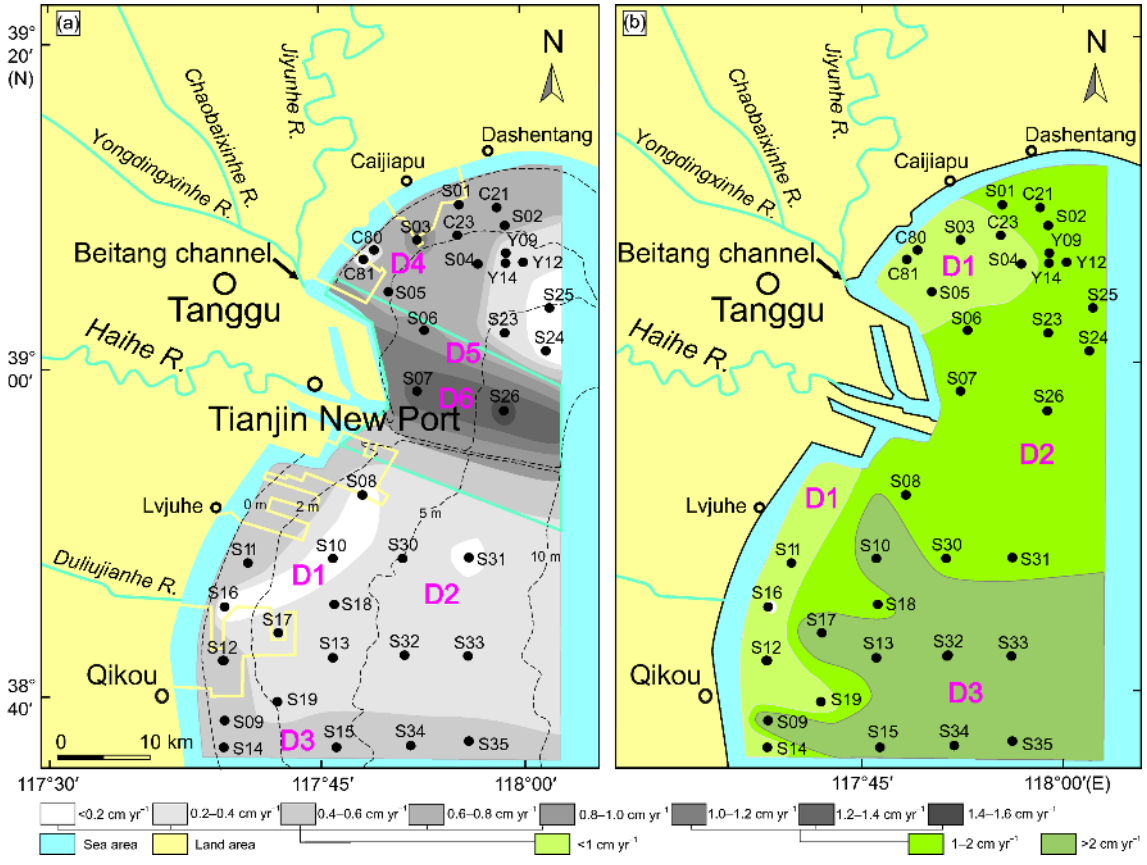

Figure 7 Distribution of sedimentation rates of Bohai Bay since 1963 (a) and 1954–1963 (b).

River and outside of the north Haihe River, where the sedimentation rates are 0.2–0.4 cm yr^{-1}. D3 is distributed in the 0–2 m water depth and southern area of the south Haihe River, where the sedimentation rates are 0.4–0.6 cm yr^{-1}. D4 is distributed in the shallowest sea area of the north Haihe River, where the sedimentation rates are 0.6–0.8 cm yr^{-1}. D5 is distributed in part area of north Haihe River, represented by sites S03 and S06, where the sedimentation rates are 0.8–1.0 cm yr^{-1}. D6 is distributed near the channel of the Tianjin New Port, represented by sites S07 and S26, where the sedimentation rates are greater than 1.2 cm yr^{-1}.

5. Discussion

5.1 Particle size and sediment supply

The particle size in north Haihe is coarser than in south Haihe, represented by higher sand content, which are the respond to the sediment dynamic and sources. There are two coastal currents from north and south, respectively in the study area. These currents converge off the shore of Tianjin and flow eastwards back to the sea (Zhao et al., 1995) (Figure 1). In south Haihe, the sediments in the intertidal flat from Haihe to Dulijianhe are mainly transported by the Haihe, but its influence cannot reach the shallow sea area based on the finer particle size distribution. The fine sediments (mainly suspended sediments) in the shallow sea area are transported by offshore currents, especially from the Yellow River. North Haihe has different coastal current and sources of material from south Haihe. The proportions of sandy components in the north are much higher than in the south area. These sediments are mainly transported by currents from Luanhe, but there is some mixing with sediments from near rivers.

The sediment particle size primarily shows a coarsening trend in the study area. Therefore, whether there is any relationship among sedimentation, river discharge, and sea level change need investigated.

5.2 Sedimentation rate in relation to sediment budget

A previous study showed that the suspended component in surface sediments from the west of the Bohai Bay is probably associated with two-way sediment transport mixing of different material elements caused by the complete changes of coastal circulation directions in different seasons based on the element characteristics (Tian et al., 2010a) and grain size characteristics (Tian et al., 2010b). Han et al. (2011) reported that the sediments in this area are mainly from the Yellow, Haihe and Luanhe Rivers based on the clay mineral assemblage. The particle size of the sediment delivered by Luanhe was coarse, with a high sandy sediment contents; the particle size of the sediments from Haihe are finer than that of the Luanhe, which have a high silt content; the sediments transported by currents are the finest and which have a high suspended sediments content.

Sediment from Haihe disperses to the north, south and out to the Bay. However, because of the blocking effect of breakwaters of the Tianjin New Port, sediment from the Haihe flows mostly southwestwards especially during the wet season in the summer and autumn due to the prevalent southeasterly or southwesterly wind of the region. The Beitang estuarine channel is the outlet of Yongdingxinhe and Jiyunhe that converge and flow into the estuary into Bohai Bay. The runoff throughout the last 50 years shows a sharp decrease after the 1960s (Table 1).

The decreasing sedimentation rates after the late 1950s closely correlate with decreasing river sediment supply, and the influence of the sediments transported by the rivers can be identified based on the distribution of the sedimentation rates after 1963 (Figure 4). In south Haihe, the sediments in the intertidal flat from Haihe to Duliujianhe are mainly transported by the Haihe, but its influence cannot reach the shallow sea area due to the finer particle size distribution (Xu, 1996) and lower sedimentation rates. In contrast, the suspended sediments in the shallow sea area are transported by offshore currents, especially from the Yellow River (Zhao et al., 1995).The north Haihe has different sources of material from the south Haihe based on particle size components of the cores. The occurrence of sandy components is much higher than in the southern area, and this material is transported mainly by currents from the Luanhe and mixed with sediments from nearby rivers (Liu, 1993). After 1915, the

Table 1 The water discharge at the Haihe River estuary, Beitang estuary and Duliujianhe estuary[a)]

Period	Beitang estuary			Haihe estuary			Duliujianhe estuary		
	Flood season	No flood season	Total	Flood season	No flood season	Total	Flood season	No flood season	Total
1950–1959			460.0			729.9			261.0
1960–1969			175.5	125.9	90.7	436.6			180.0
1970–1979			257.3	85.9	14.9	100.9	38.0	2.0	40.0
1980–1989	58.1	16.7	75.9	13.5	3.5	17.0	0.7	0.0	0.7
1990–1999	117.1	21.3	141.7	21.4	6.9	28.4	21.6	7.4	29.0

a) Lei et al., 2007. Unit: 10^8 m^3

Luanhe estuary migrated northward, further away from Chengtougu-Dashentang. Consequently, the quantity of coarse sediment transported from Luanhe decreased sharply (Wang F et al., 2014). The sedimentation rates of the northern Haihe River are higher than those in the southern area because the sediments from eastern sea area were transported to this area by stronger currents.

5.3 Sedimentation rates and implication

Bi et al. (2013) suggested that the increase in the rate of sea level rise in the Tianjin area is due to the major coastal development, especially the coastal use, reducing the volume of Bohai Bay. Essentially that the incoming tide has the same volume but has less area to flood over. Therefore, the sea-water level is forced up. The effect is amplified if there is a reduction in sediment supply, and no increase in accommodation space through land subsidence. Ericson et al. (2006) suggested that the contemporary net rate of sea level rise is defined as the combination of eustatic sea level rise, the natural gross rate of fluvial sediment deposition and subsidence. This can be accelerated locally by subsidence, and by groundwater and hydrocarbon extraction. In addition, reduced accretion of fluvial sediment, for example as the result of upstream siltation in artificial impoundments and channel flow reduction, contribute significantly to relative sea level rise in nearly 70% of deltas. Therefore, the rate of sedimentation in the coastal zone is an important factor when considering the local controls influencing relative sea level rise.

Compared with the regional average before 1963, the sedimentation rates are higher, and only a small area located on core S31 in the south Haihe, core S25, and Y14 in the north Haihe are lower. However, after 1963, the regional average sedimentation rate decreased sharply in most of the study area. Including the area of 0–10 m water depth in the south Haihe, and part of the area in 0 m water depth near Dashentang. In addition, we note that the area of 5 m water depth near core S25 and Y12 in the north Haihe the rates are lower than the mean local sea level rising rates.

The coastline of the study area is now dominated by artificial structures. After 2007, most of the supratidal zones in the area and part of the shallow sea area have been reclaimed, and the width of tidal flats has decreased due to human activities (Figure 1). The intertidal flat has become narrower and steeper in our study area (Wang et al., 2010), with the same results in Jiangsu coast, Jiaozhou Bay China, following sequential reclamations (Wang et al., 2012; Wang Y P et al., 2014) and other rocky shorelines being reclaimed. Human activity has also led to the formation of many intrusive coastal features, like large concrete constructions within the intertidal zone and the nearshore shallow sea area. This type of engineering restricts the flow and movement of sea water during high-tide, and slows the natural drainage of extreme water level events.

In the next 30 years, the sea level of Tianjin is expected to rise 105–195 mm (SOA, 2015); the increase rate is 3.5–6.5 mm yr^{-1}. The observed average sedimentation rates since the 1950s can keep pace with sea level rises , but comparison of the accumulation rates in 1954–1963 and 1963–2007 revealed an obvious decrease in sediment deposition. The observed decrease in sediment deposition is significant and gives reason for concern as it may be the common sign of sedimentation deficiency, which could threaten these artificial constructions. For example, the reclamation of both inshore and offshore intertidal areas would impact the near-shore accommodation space and increase tidal flows. An increase in tidal energy coupled with rapidly rising sea level could increase the probability of coastal hazards, e.g., severe erosion (Zhu et al., 2016), and this situation will require urgent countermeasures to maintain the coastline.

As the flow of sediments from the land into the sea is reduced, the study shows that many of the world's deltas are becoming more vulnerable to flooding and inundation. This results from combination of impacts from the exploitation of natural resources (such as gas and oil), the trapping of sediment in reservoirs upstream and floodplain engineering and the steady upward trend of global sea level (Syvitski, 2012). One result is many of the coasts around the world will face the same situation as Bohai Bay of rising relative sea level and decreasing regional sediment supply. Whether sedimentation can keep pace with the sea level is important for the future of these areas. Our study shows that sedimentation cannot keep pace with the sea level increase since the 1960s in Bohai Bay. This result is also the case for many other shallow seas, especially if the sea level continues to rise rapidly, as indicated by climate change.

6. Conclusions

In the shallow sea area of Bohai Bay, the sedimentation rates before the last 50 years have generally kept pace with, or were slightly higher than, the average rate of sea level rising, 3.4 mm yr^{-1}. After the 1960s, however, the sedimentation rates decreased sharply because all the rivers entering the bay were dammed, and the sediments being delivered to the coastal zone decreased, leading to the sedimentation rates of most areas being lower than that of the sea level rising. Consequently, the particle size shows a coarsening trend in the shallow sea area of the bay, which was the response to the decreasing river sediment delivery and rising sea level.

The observed decrease in sediment deposition is significant and gives reason for concern as it may be a common sign of sedimentation deficiency, which could threaten these

highly invested coastlines, especially the artificial constructions, in the case of a rapidly rising sea level. This result is also the case for many other bays and shallow seas, especially if the sea level continues to rise rapidly in this century.

Acknowledgements *We thank Prof. Chen Z. Y. (East China Normal University) and anonymous reviewers, who gave many constructive suggestions. We also thank Mr. Pei Y. and Shang Z., who contributed to fieldwork and sample preparation respectively. We are also deeply indebted to Mr. Xia Weilan (Key Laboratory of Lake Sedimentation & Environment, Chinese Academy of Sciences) and Mrs. Wu Liangying (Young Sediments Dating Laboratory, Tianjin Institute of Geology and Mineral Resources), who kindly helped measure ^{210}Pb and ^{137}Cs activity, and Mr. Deng Shiqun (Grain Size Analyzing Laboratory of the Tianjin Center of Geological Survey), who kindly helped measure grain size. This work was supported by the National Natural Science Foundation of China (Grant No. 41206069) and the China Geological Survey, CGS (Grant No. 121201006000182401).*

References

Andersen T J, Mikkelsen O A, Møller A L, Morten Pejrup A L. 2000. Deposition and mixing depths on some European intertidal mudflats based on and activities. Cont Shelf Res, 20: 1569–1591

Bi X L, Lu Q S, Pan X B. 2013. Coastal use accelerated the regional sea-level rise. Ocean Coast Manage, 82: 1–6

Blum M D, Roberts H H. 2009. Drowning of the Mississippi Delta due to insufficient sediment supply and global sea-level rise. Nat Geosci, 2: 488–491

Callaway J C, DeLaune R D, Patrick Jr W H. 1996. Chernobyl ^{137}Cs used to determine sediment accretion rates at selected northern European coastal wetlands. Limnol Oceanogr, 41: 444–450

Cambray R S, Playford K, Lewis G N J, Carpenter R C. 1989. Radioactive fallout in air and rain: Results to the end of 1987. ReportA.E.R.E.-R 13226 DOE/RW/89/059. Environmental and Medical Sciences Division. Harwell: Harwell Laboratory. 20

China Communications First Design Institute of Navigation Engineering and National Marine Data and Information Service. 2006. Waves, tides and high water by storm surges analysis report of Tianjin New Port, Eastern Port. 70

Delaune R D, Patrick W H, Buresh R J. 1978. Sedimentation rates determined by ^{137}Cs dating in a rapidly accreting salt marsh. Nature, 275: 532–533

Ericson J P, Vorosmarty C J, Dingman S L, Ward L G, Meybeck M. 2006. Effective sea-level rise and deltas: Causes of change and human dimension implications. Glob Planet Change, 50: 63–82

Gehrels W R, Marshall W A, Gehrels M J, Larsen G, Kirby J R, Eiríksson J, Heinemeier J, Shimmield T. 2006. Rapid sea-level rise in the North Atlantic Ocean since the first half of the nineteenth century. Holocene, 16: 949–965

Goodbred Jr S L, Kuehl S A. 1998. Floodplain processes in the Bengal Basin and the storage of Ganges-Brahmaputra river sediment: An accretion study using ^{137}Cs and ^{210}Pb geochronology. Sediment Geol, 121: 239–258

Han Z Z, Zhang J Q, Zou H, Yi W H, Li M. 2011. Characteristics and provenance of clay mineral assemblage of sediments from the northern part of the Bohai Bay (in Chinese with English abstract). Period Ocean Univ China, 11: 95–102

He Q X. 2006. Marine Sedimentary Geology of China. Beijing: Ocean Press. 503

Hormann V, Fischer H W. 2013. Estimating the distribution of radionuclides in agricultural soils—Dependence on soil parameters. J Environ Radioact, 124: 278–286

Hu S X, Qi J. 2000. Shrink of estuaries in Haihe basin and its effects on the flood disaster (in Chinese with English abstract). Haihe River Hydraul, 1: 11–13

IPCC. 2013. 5th Report-Climate Change 2013 The Physical Science Basis. http://www.ipcc.ch/report/ar5/wg1/

Irabien M J, Cearreta A, Leorri E, Gómez J, Viguri J. 2008. A 130 year record of pollution in the Suances estuary (southern Bay of Biscay): Implications for environmental management. Mar Pollut Bull, 56: 1719–1727

James P M, Syvitski A J, Kettner I O, Hutton E W H, Hannon M T, Brakenridge R. 2009. Sinking deltas due to human activities. Nat Geosci, 2: 681–686

Jha S K, Chavan S B, Pandit G G, Sadasivan S. 2003. Geochronology of Pb and Hg pollution in a coastal marine environment using global fallout ^{137}Cs. J Environ Radioact, 69: 145–157

Kabdyrakova A M, Lukashenko S N, Mendubaev A T, Kunduzbayeva A Y, Panitskiy A V, Larionova N V. 2018. Distribution of artificial radionuclides in particle-size fractions of soil on fallout plumes of nuclear explosions. J Environ Radioact, 186: 45–53

Lei K, Meng W, Zheng B H, Hou X M, Sun Y C. 2007. Variations ofwater and sediment discharges to the western coast of BohaiBay and the environmental impacts (in Chinese with English abstract). Acta Sci Circum, 12: 2052–2059

Le Roux G, Marshall W A. 2010. Constructing recent peat accumulation chronologies using atmospheric fall-out radionuclides. Mires and Peat, 7: 1–14

Li J F, Kang H, Wang H, Pei Y D. 2007. Modern geological action and discussion of influence factors on the west coast of Bohai Bay, China (in Chinese with English abstract). Geol Sur Res, 4: 295–301

Li X B, Sun X Y, Wang S F, Ye F J, Li Y J, Li X Y. 2011. Characteristic analysis of Tianjin offshore tide (in Chinese with English abstract). Mar Sci Bull, 13: 40–49

Liu F S. 1993. Development characteristics of modern Luanhe River delta (in Chinese with English abstract). Mar Sci Bull, 1: 54–60

Marshall W A, Gehrels W R, Garnett M H, Freeman S P H T, Maden C, Xu S. 2007. The use of 'bomb spike' calibration and high-precision AMS ^{14}C analyses to date salt-marsh sediments deposited during the past three centuries. Quat Res, 68: 325–337

Martínez M L, Intralawan A, Vázquez G, Pérez-Maqueo O, Sutton P, Landgrave R. 2007. The coasts of our world: Ecological, economic and social importance. Ecol Econ, 63: 254–272

McManus J. 1988. Grain size determination and interpretation. In: Tucker M E, ed. Techniques in Sdimentology. Oxford: Blackwell. 63−85

Mishra U C, Lalit B Y, Sethi S K, Shukla V K, Ramachandran T V. 1975. Some observations based on the measurements on fresh fallout from the recent chinese and french nuclear explosions. J Geophys Res, 80: 5045–5049

Qin Y S, Zhao Y Y, Chen L R, Zhao S L. 1990. Geology of Bohai Sea (in Chinese). Beijing: China Ocean Press. 3–200

Radakovitch O, Charmasson S, Arnaud M, Bouisset P. 1999. ^{210}Pb and Caesium accumulation in the rhône delta sediments. Estuar Coast Shelf Sci, 48: 77–92

Sardá R, Avila C, Mora J. 2005. A methodological approach to be used in integrated coastal zone management processes: The case of the Catalan Coast (Catalonia, Spain). Estuar Coast Shelf Sci, 62: 427–439

SOA. 2017. Sea Level Bulletin 2016. State Oceanic Administration People's Republic of China. SOA Web site: http://www.coi.gov.cn/gongbao/haipingmian/

SOA. 2015. Sea Level Bulletin 2014. State Oceanic Administration People's Republic of China. SOA Web site: http://www.coi.gov.cn/gongbao/haipingmian/

Su C C, Huh C A. 2002. ^{210}Pb, ^{137}Cs and ^{239,240}Pu in East China Sea sediments: Sources, pathways and budgets of sediments and radionuclides. Mar Geol, 183: 163–178

Su S W, Shang Z W, Wang F, Wang H. 2011. Holocene chenier: Spatial and temporal distribution and sea level indicators in Bohai Bay (in Chinese with English abstract). Geol Bull China, 9: 1382−1395

Syvitski J. 2012. Vulnerability of coastlines—How do environmental changes affect coastlines and river deltas? Pages news: Paired per-

spectives on global change, 1: 34–35
Tianjin Bureau of Statistics. 2013. 2012 Population development in Tianjin. http://www.chinanews.com/gn/2013/04-04/4703890.shtml
Tian L Z, Pei Y D, Shang Z W and Wang H. 2010a. Elements characteristics of the suspended component in surface sediments from the west Bohai Bay the provenance implication (in Chinese with English abstract). Mar Geol Quat Geol, 1: 9–15
Tian L Z, Geng Y, Pei Y D. 2010b. The grain-size characteristics and sediment mixing pattern of surface sediment from the westernBohai Bay, China (in Chinese with English abstract). Geol Bull China, 5: 668–674
Wang F, Li J F, Chen Y S, Fang J, Zong Y Q, Shang Z W, Wang H. 2015. The record of mid-Holocene maximum landward marine transgression in the west coast of Bohai Bay, China. Mar Geol, 359: 89–95
Wang F, Pei Y D, Li J F, Shang Z W, Fan C F, Tian L Z, Song M Y, Geng Y, Wang H. 2010. The status elevation of tidal flat: A potential factor influencing the andTianjin Binhai New Area safety (in Chinese with English abstract). Geol Bull China, 4: 682–687
Wang F, Wang H, Zong Y, Andersen T J, Pei Y D, Tian L Z, Li J F, Shang Z W. 2014. Sedimentary dynamics along the West Coast of Bohai Bay, China, during the Twentieth Century. J Coast Res, 294: 379–388
Wang F, Tian L Z, Jiang X Y, Li J F, Yang B, Yuan H F, Wang H. 2016a. Local ^{137}Cs reference profile on Bohai Bay: Implications, methods and initial results. Geol Bull China, 10: 1622–1629
Wang F, Yang B, Tian L Z, Li J F, Shang Z W, Chen Y S, Jiang X Y, Yang J L, Wang H. 2016b. The choice of CIC and CRS models of $^{210}Pb_{exc}$ dating for tidal flat area (in Chinese with English abstract). Earth Sci, 6: 971–981
Wang F, Zong Y Q, Li J F, Tian L Z, Shang Z W, Chen Y S, Jiang X Y, Yang J L, Yang B, Wang H. 2016c. Recent Sedimentation Dynamics Indicated by $^{210}Pb_{exc}$ and ^{137}Cs Records from the Subtidal Area of Bohai Bay, China. J Coast Res, 318: 416–423
Wang H, Chen Y S, Tian L Z, Li J F, Pei Y D, Wang F, Shang Z W, Fan C F, Jiang X Y, Su S W, Wang H. 2011. Holocene cheniers and oyster reefs in Bohai Bay: Palaeoclimate and sea level changes (in Chinese with English abstract). Geol Bull China, 9: 1405−1411
Wang H. 2003. Geo-environmental changes on the Bohai Bay muddy coast (II): Result and discussions (in Chinese with English abstract). Quat Sci, 4: 393–403
Wang H, Liu K X, Fan W J, Fan Z H. 2013. Data uniformity revision and variations of the sea level of the western Bohai Sea. Mar Sci Bull, 3: 256–264
Wang Y P, Gao S, Jia J J, Thompson C E L, Gao J H, Yang Y. 2012. Sediment transport over an accretional intertidal flat with influences of reclamation, Jiangsu coast, China. Mar Geol, 291-294: 147–161
Wang Y P, Gao S, Jia J, Liu Y, Gao J. 2014. Remarked morphological change in a large tidal inlet with low sediment-supply. Cont Shelf Res, 90: 79–95
Wei T Y, Chen Z Y, Duan L Y, Gu J W, Saito Y, Zhang W G, Wang Y H, Kanai Y. 2007. Sedimentation rates in relation to sedimentary processes of the Yangtze estuary, China. Estuar Coast Shelf Sci, 71: 37–46
Xu L M. 1996. Analysis on the washing and silting characteristics of fine sand beach at the west of Bohai Gulf (in Chinese with English abstract). Port Eng Technol, 2: 9–14
Xue Z, Feng A, Yin P, Xia D. 2009. Coastal erosion induced by human activities: A northwest Bohai Sea case study. J Coast Res, 253: 723–733
Zhang W, Ruan X, Zheng J, Zhu Y, Wu H. 2010. Long-term change in tidal dynamics and its cause in the Pearl River Delta, China. Geomorphology, 120: 209–223
Zhao B R, Zhuang G W, Cao D M, Lei F H. 1995. Circulation, tidal residual currents and their effects on the sedimentations in the Bohai Sea (in Chinese with English abstract). Oceanol Limnol Sin, 5: 466–473
Zhong X B, Kang H. 2002. Recent geo-environmental changes in the Bohai Bay coast (in Chinese with English abstract). Quat Sci, 2: 131–135
Zhu Q G, Wang Y P, Ni W F, Gao J H, Li M L, Yang L, Gong X L, Gao S. 2016. Effects of intertidal reclamation on tides and potential environmental risks: A numerical study for the southern Yellow Sea. Environ Earth Sci, 75: 1472

(Responsible editor: Huayu LU)